Electronic Supplementary Information

A new hybrid material of polyoxovanadate-Cu complex with V···H interactions and dual aqueous phase sensing properties for picric acid as well as Pd^{2+}: X-ray, magnetic and theoretical studies, and mechanistic insights of sensing†

Mukul Raizada[a]*, Farasha Sama [a], Mo Ashafaq[a], M. Shahid[a]*, Musheer Ahmad[b], Zafar A. Siddiqi [a]*

[a]*Department of Chemistry, Aligarh Muslim University, Aligarh-202002, India*
[b]*Department of Applied Chemistry, Aligarh Muslim University, Aligarh-202002, India*
* Corresponding authors, E-mail: zafarasiddiqi@gmail.com, shahid81chem@gmail.com, mukulraizada1@gmail.com

Formula for calculating the percentage of Picric acid fluorescence intensity quenching:

$$(Io-I)/Io \times 100\%$$

Where, Io = initial fluorescence intensity,

I = intensity of **1** containing PA solution.

Reference: (a) S. Pramanik, C. Zheng, X. Zhang, T. J. Emge and J. Li, *J. Am. Chem. Soc.*, 2011, **133**,4153; (b) D. Banerjee, Z. Hu and J. Li, *Dalton Trans.*, 2014, **43**, 10668.

Stern-Volmer equation:

$$I_0/I = K\text{SV}[A] + 1$$

Where, I_0 = fluorescent intensity of **1** before the addition of the analyte

I = fluorescent intensity after the addition of the respective analyte

K_{SV} = Stern-Volmer constant

[A] = molar concentration of the analyte (M^{-1}).

Table S1. Bond valence sum calculation of Vanadium (V) oxidation state in the crystal structure of **1** [a]

Atom	V^{V}	V^{IV}	V^{III}
V0	***4.985***	4.735	4.239
V1	***4.948***	4.701	4.208
V2	***5.041***	4.789	4.287
V3	***4.920***	4.674	4.184
V4	***4.964***	4.716	4.221
V6	***4.985***	4.736	4.239
V7	***4.953***	4.706	4.212
V8	***4.991***	4.741	4.244
V9	***4.948***	4.701	4.208
V10	***5.023***	4.776	4.228

[a] The Values in ***bold italicised underlined*** are the closest to the charge for which it was calculated; the nearest whole number can be taken as the oxidation state of that atom.

Table S2. Distances and angles of non-covalent interaction in **1**.

D–H···A	d(D–H)	d(H···A)	d(D···A)	∟(DHA)
C13–H13···V0AA	0.930	3.086	3.861	141.87
C18–H18···V4	0.930	3.147	3.955	146.30
C4–H4A···V9	0.969	3.161	4.028	149.63
C11–H11A···V3	0.970	3.180	4.043	149.04
N5–C9···O11	1.513	3.193	4.033	113.02
C23–H23···O18	0.930	2.377	3.177	143.98
C24–H24···O28	0.930	2.465	3.272	145.12
C28–C29···C22	1.386	3.262	3.508	88.40
C9–H9A···O11	0.971	2.654	3.193	115.46
C18–H18···O16	0.930	2.171	3.092	170.72
C23–H23···O18	0.930	2.377	3.177	143.98
C5–H5B···O3	0.970	2.610	3.213	120.55

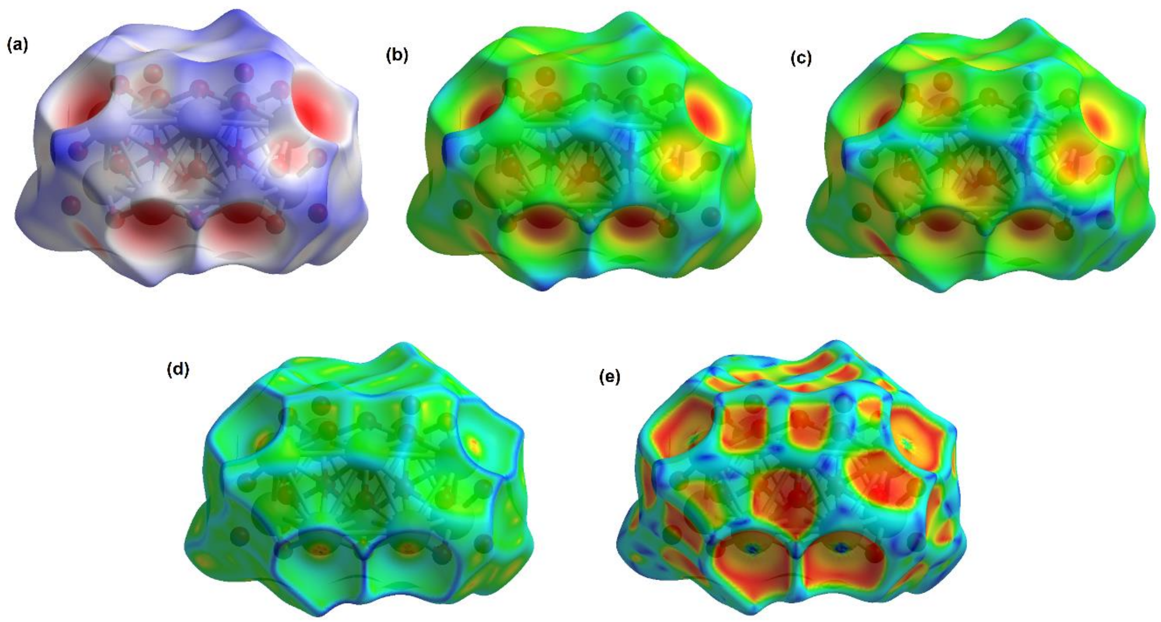

Fig. S1: (a) Hirshfeld surface of 1 mapped with d_{norm} (a), d_i (b), d_e (c), shape index (d) and curvedness (e) for decavanadate unit.

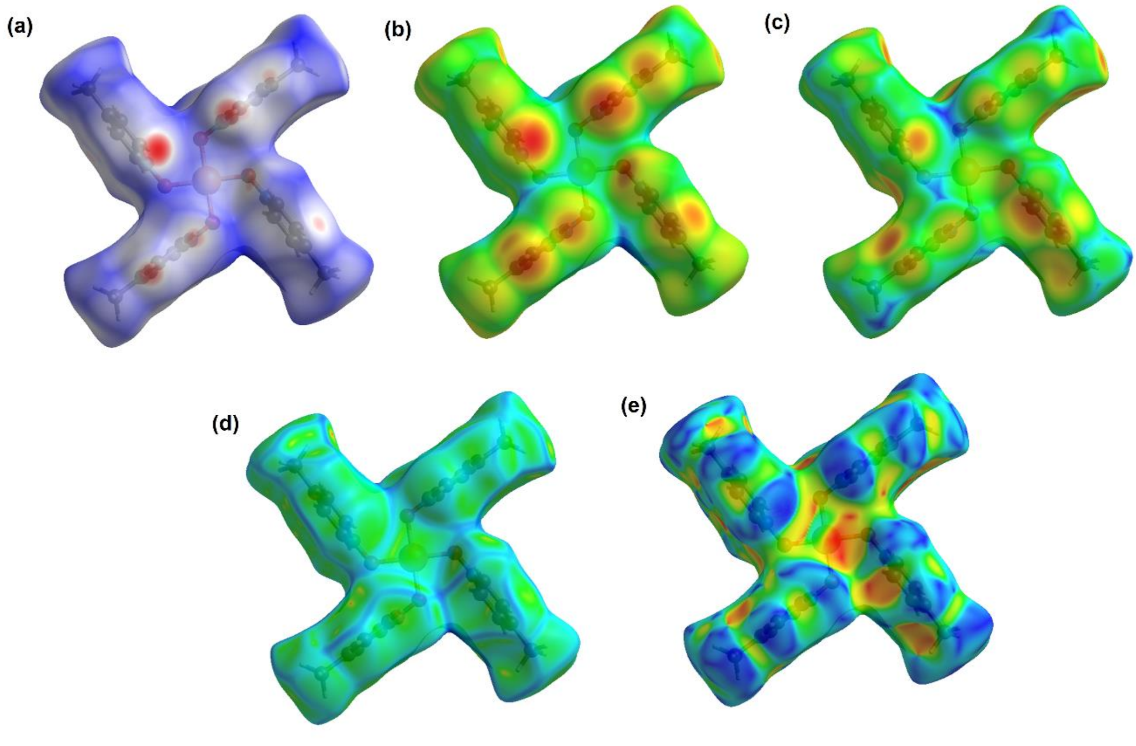

Fig. S2: (a) Hirshfeld surface of 1 mapped with d_{norm} (a), d_i (b), d_e (c), shape index (d) and curvedness (e) for copper unit.

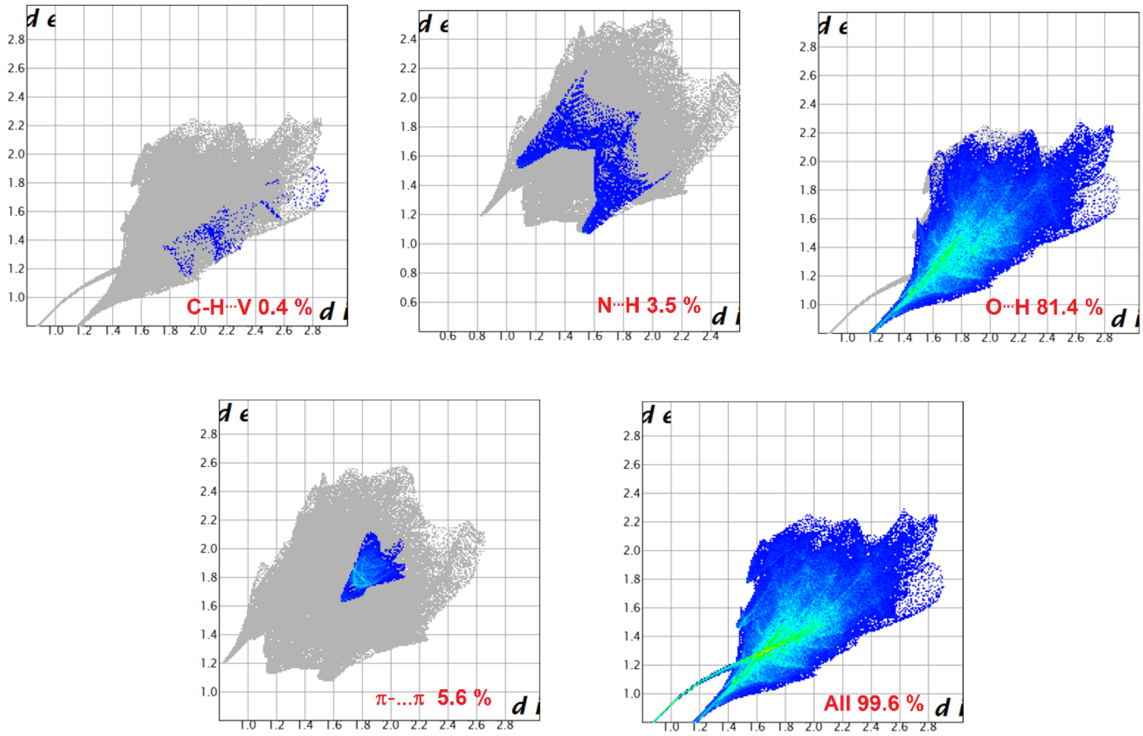

Fig. S3: 2D Fingerprint plots for various interactions present in the $V_{10}O_{28}$-Cu-pyno-NEt unit.

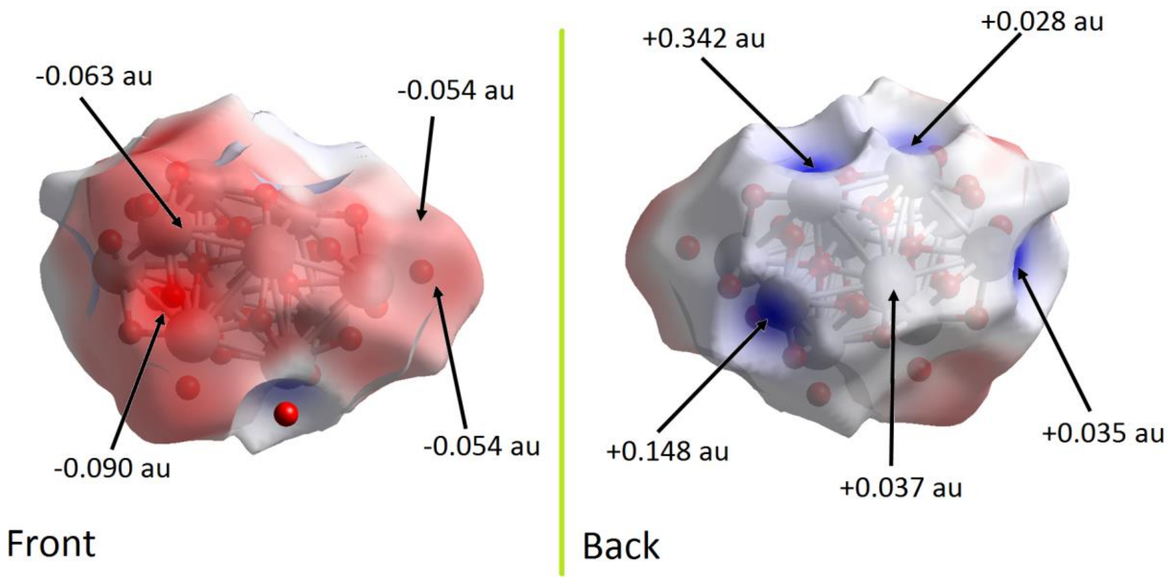

Fig. S4: Front and back views of the electrostatic potential (ESP) mapped over the Hirshfeld surface for $V_{10}O_{28}$-Cu-pyno-NEt over the range −0.136 au (red) through 0.000 (white) to +1.185 au (blue).

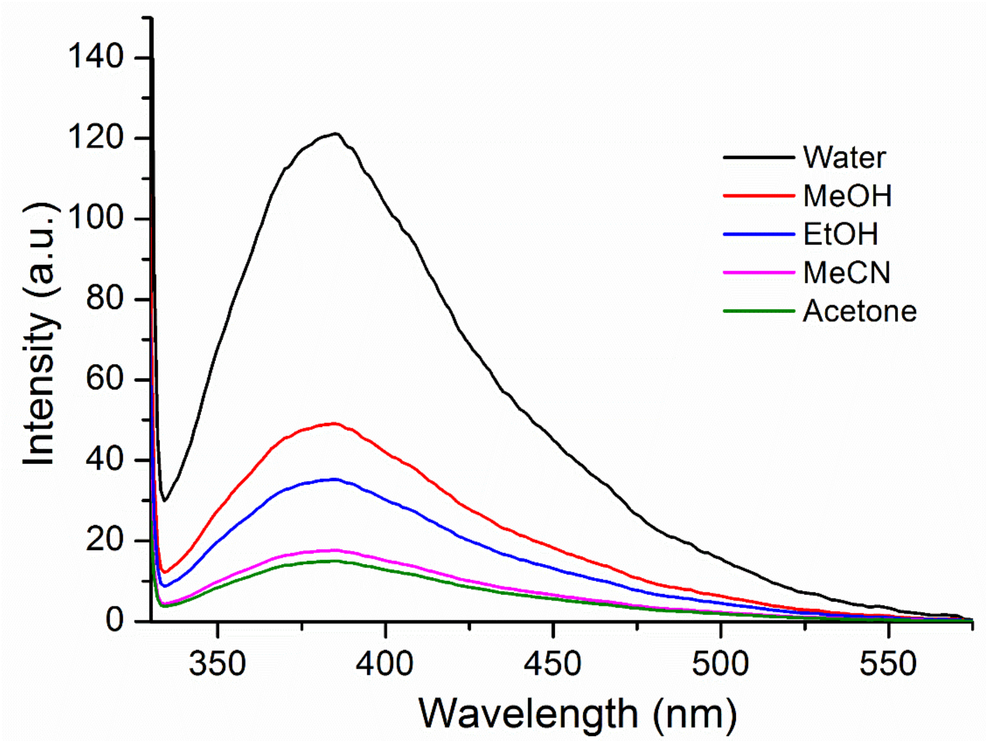

Figure S5: Emission spectrum of **1** dispersed in different solvents upon excitation at 304 nm.

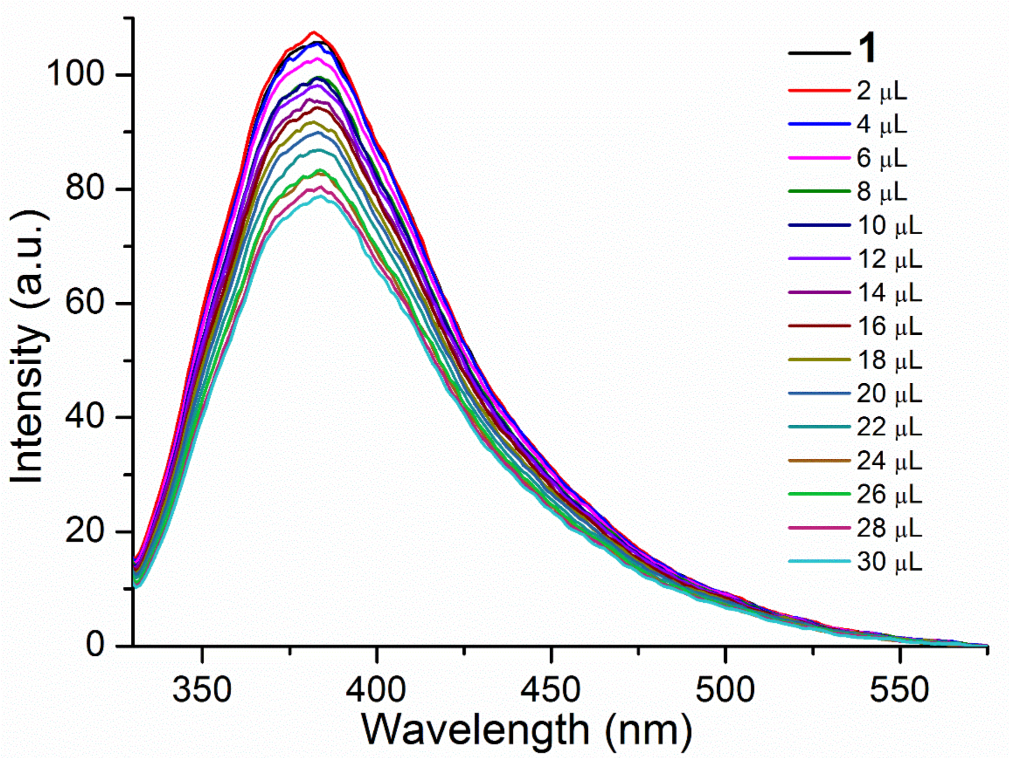

Fig. S6: The change in fluorescence intensity of **1** upon incremental addition of NB solution in Water.

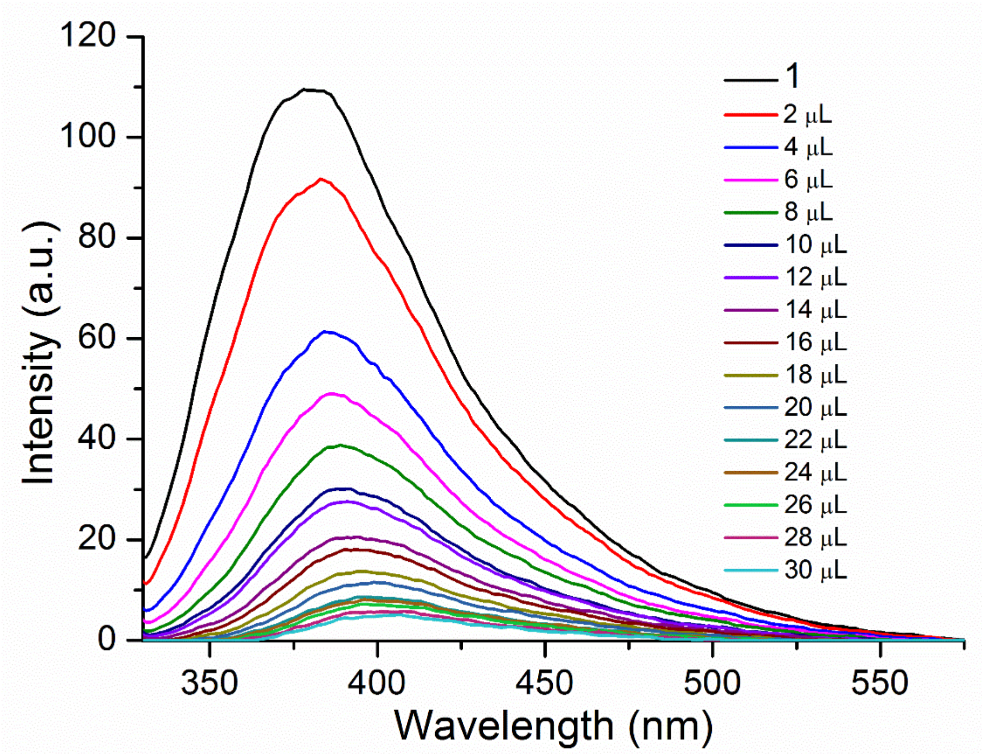

Fig. S7: The change in fluorescence intensity of **1** upon incremental addition of MNP solution in Water.

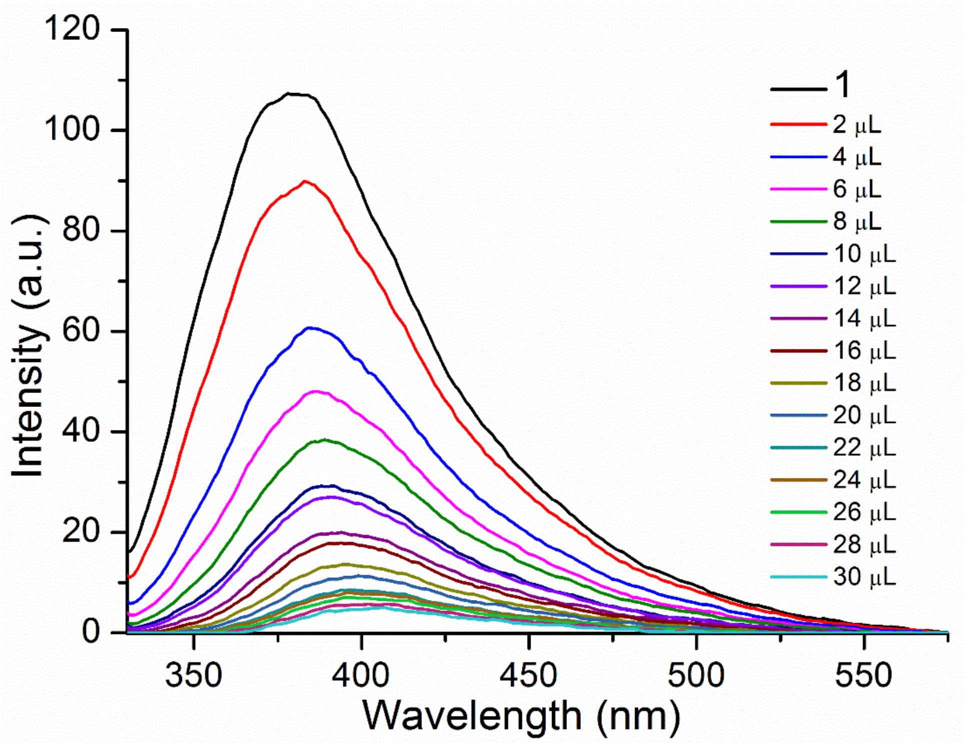

Fig. S8: The change in fluorescence intensity of **1** upon incremental addition of PNP solution in Water.

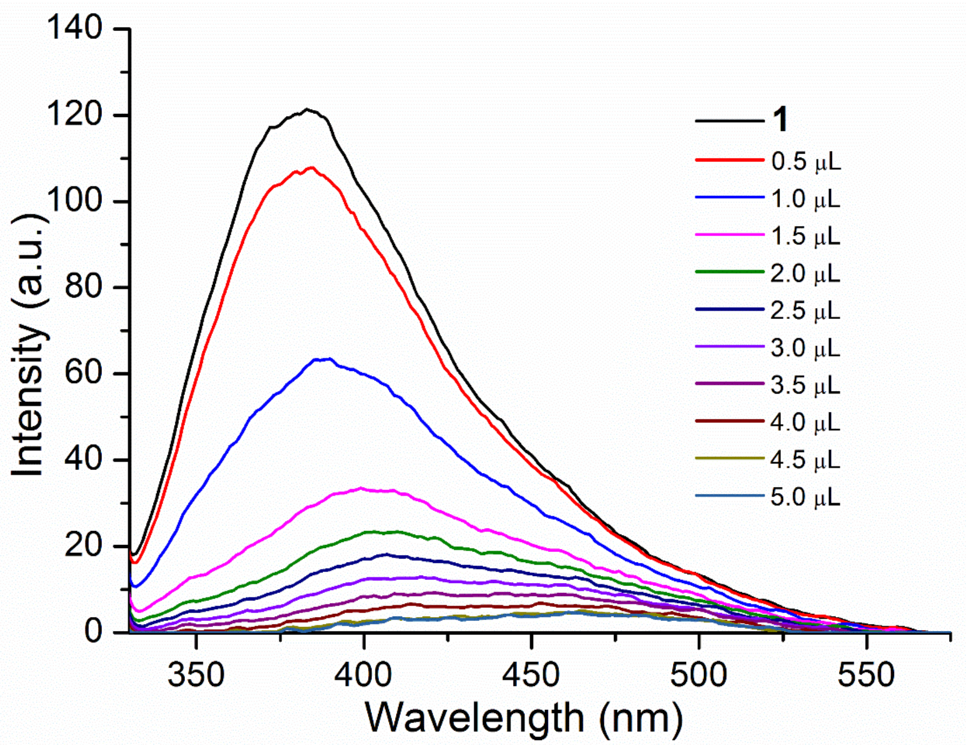

Fig. S9: The change in fluorescence intensity of **1** upon incremental addition of 2,4-DNP solution in Water.

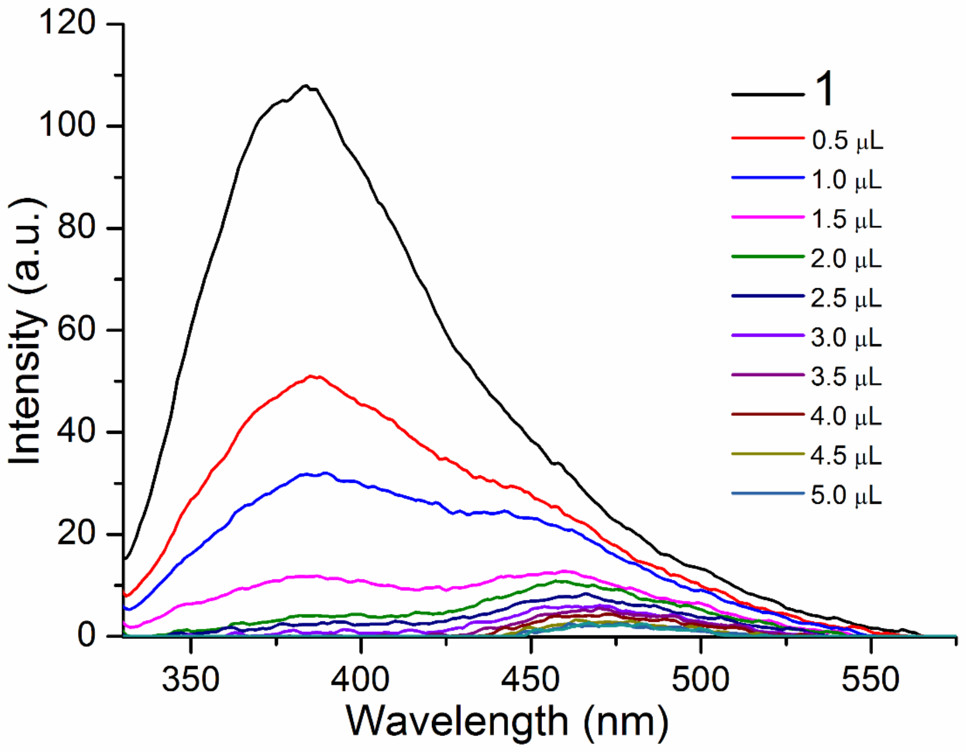

Fig. S10: The change in fluorescence intensity of **1** upon incremental addition of PA solution in Water.

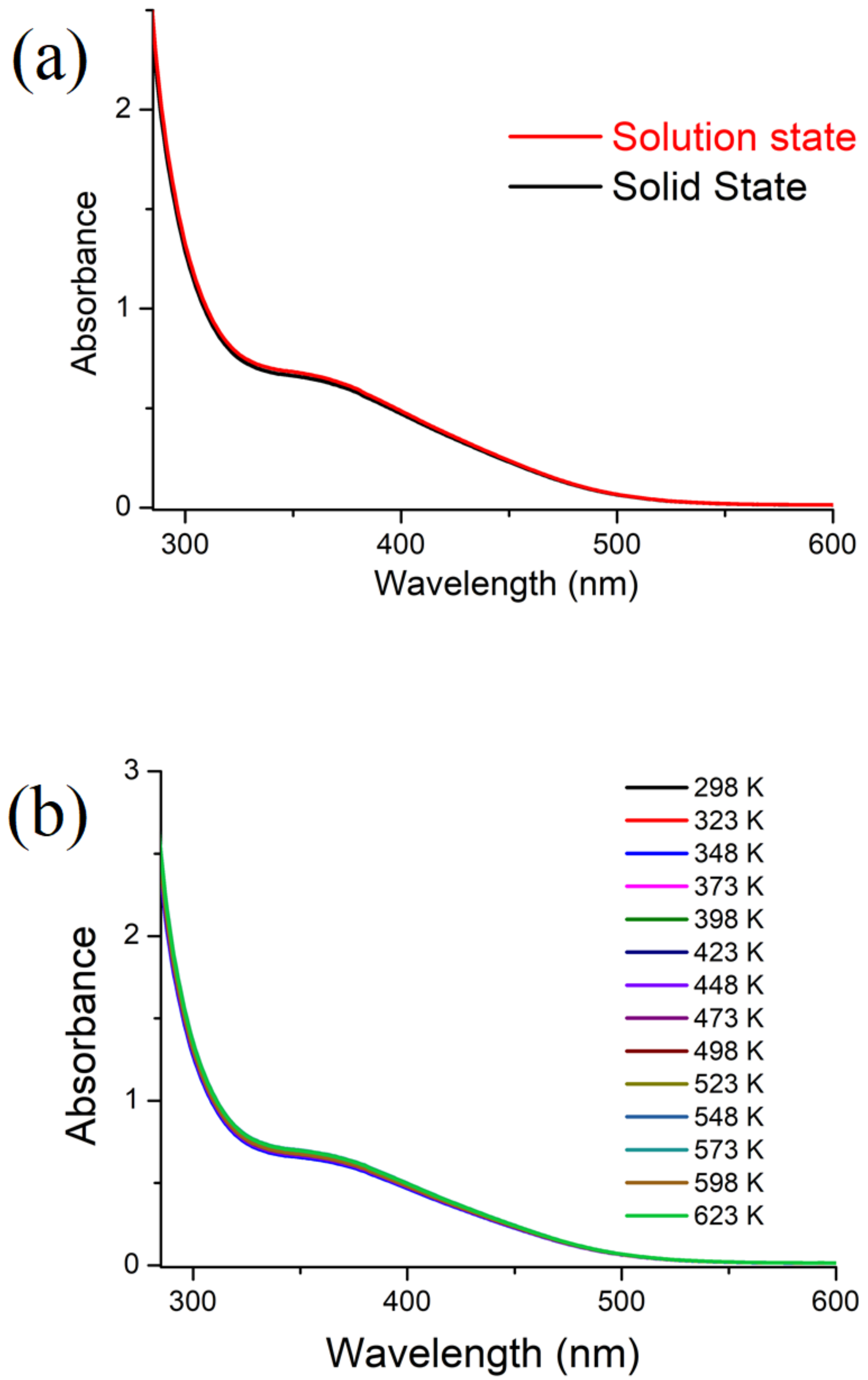

Fig. S11: (a) Solid and solution (water) state UV-Visible spectra of **1.** (b) UV-Visible spectra at different temperature.

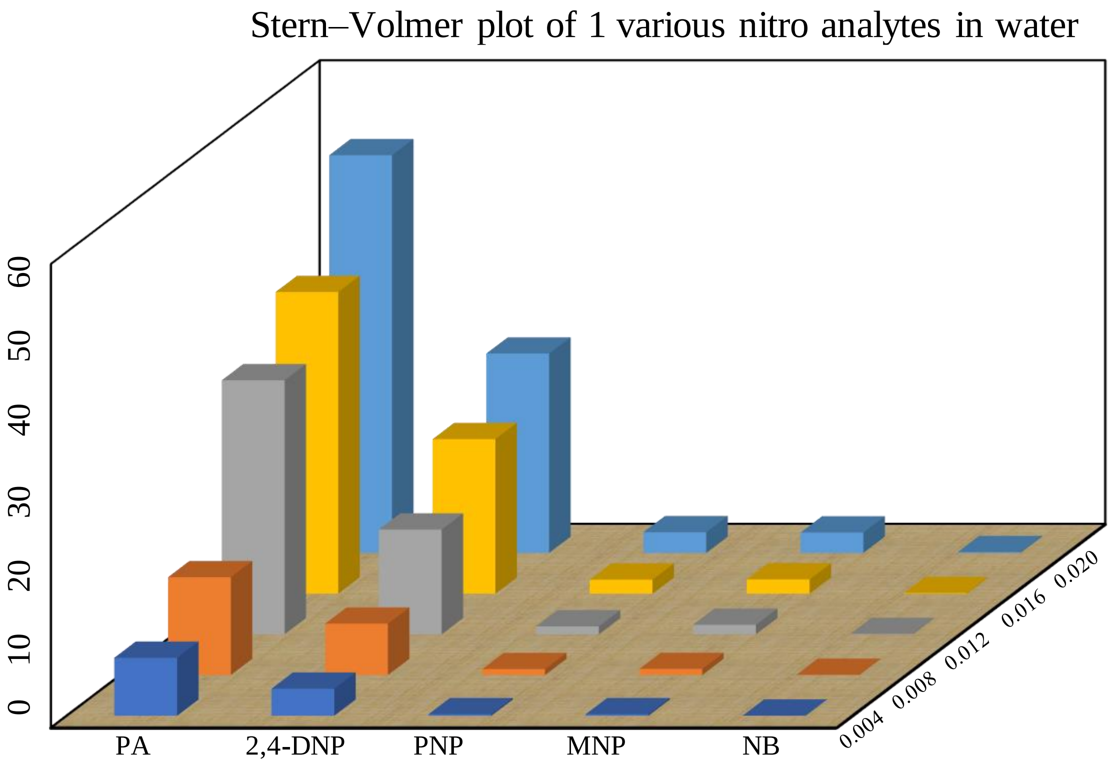

Fig. S12: 3D representation of Stern-Volmer (SV) plots of **1** for various NACs.

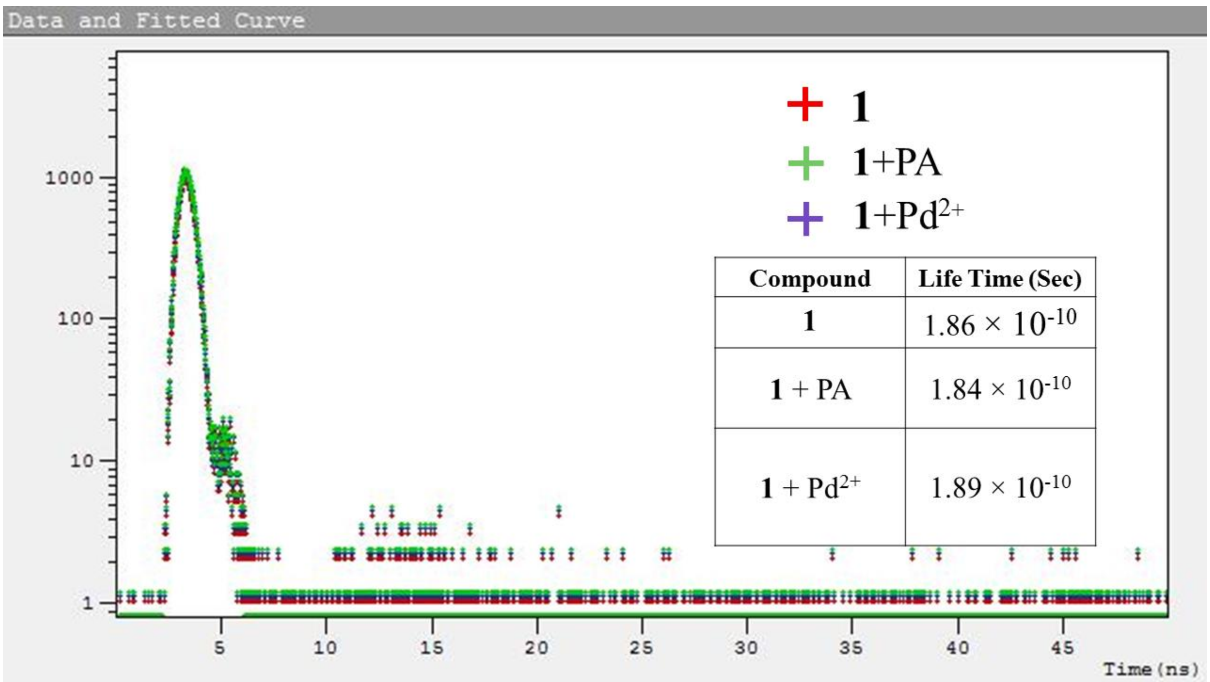

Compound	Life Time (Sec)
1	1.86×10^{-10}
1 + PA	1.84×10^{-10}
1 + Pd^{2+}	1.89×10^{-10}

Fig. S13: Fluorescence decay profile of **1** in the presence and absence of PA and Pd^{2+} solution.

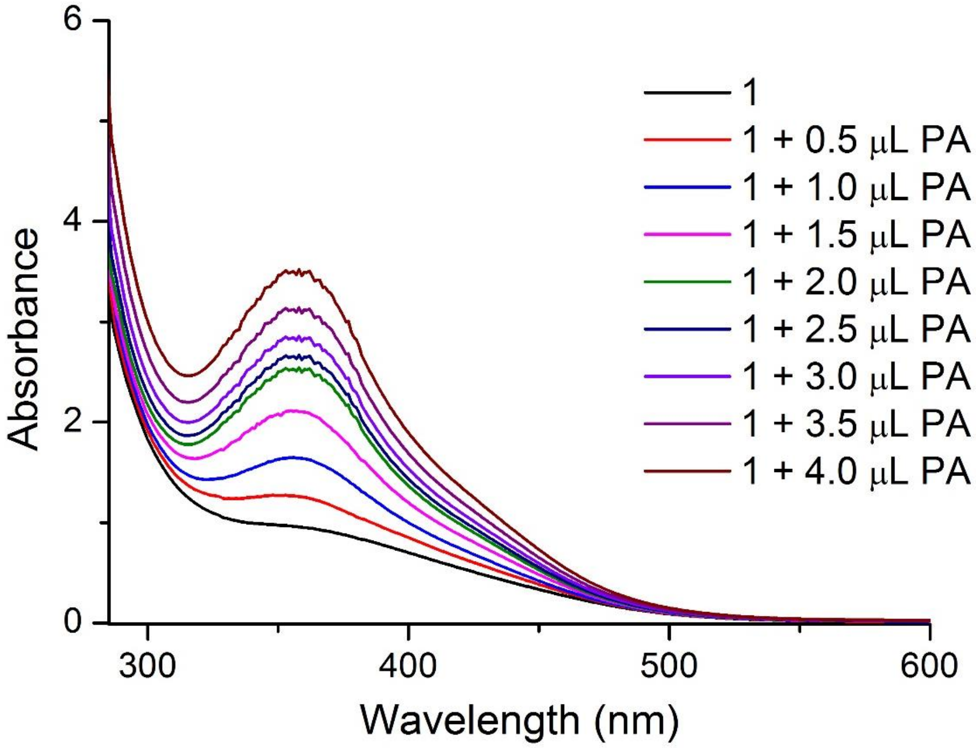

Fig. S14: UV-vis spectra of **1** upon gradual addition of PA showing spectral change with the appearance of new band at 356 nm.

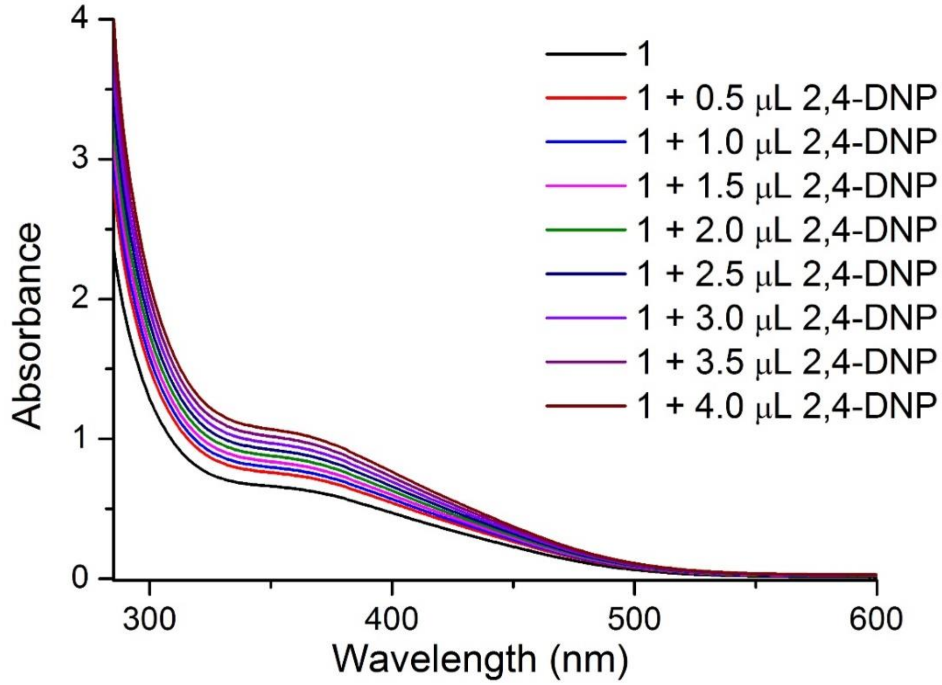

Fig. S15: UV-vis spectra of **1** upon gradual addition of 2,4-DNP showing spectral change with the appearance of new band at 366 nm.

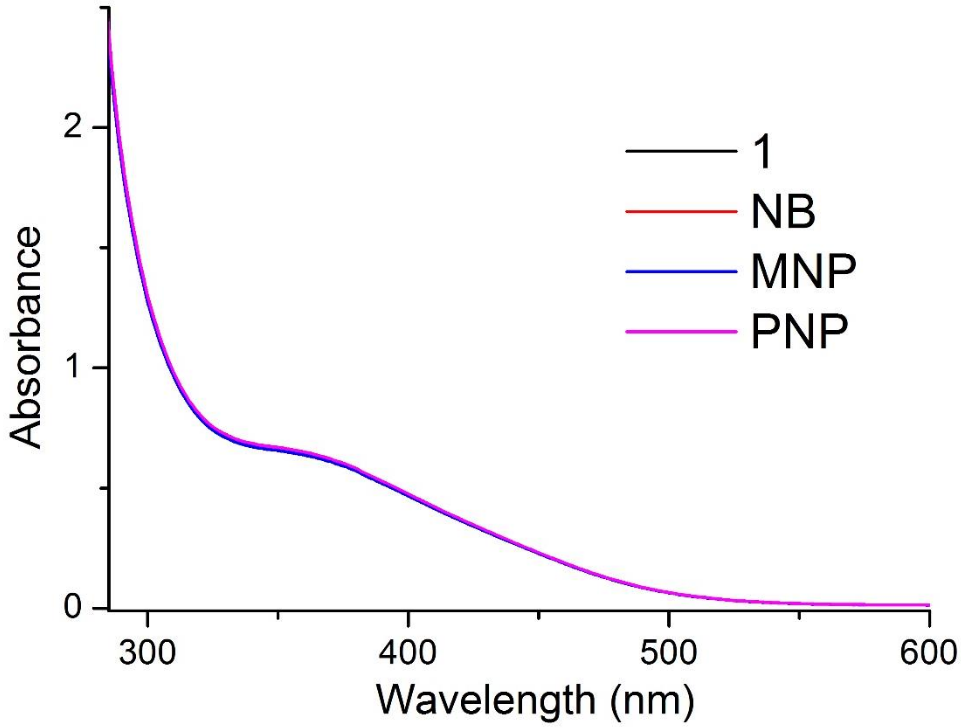

Fig. S16: UV-vis spectra of **1** in the presence of different nitro analytes.

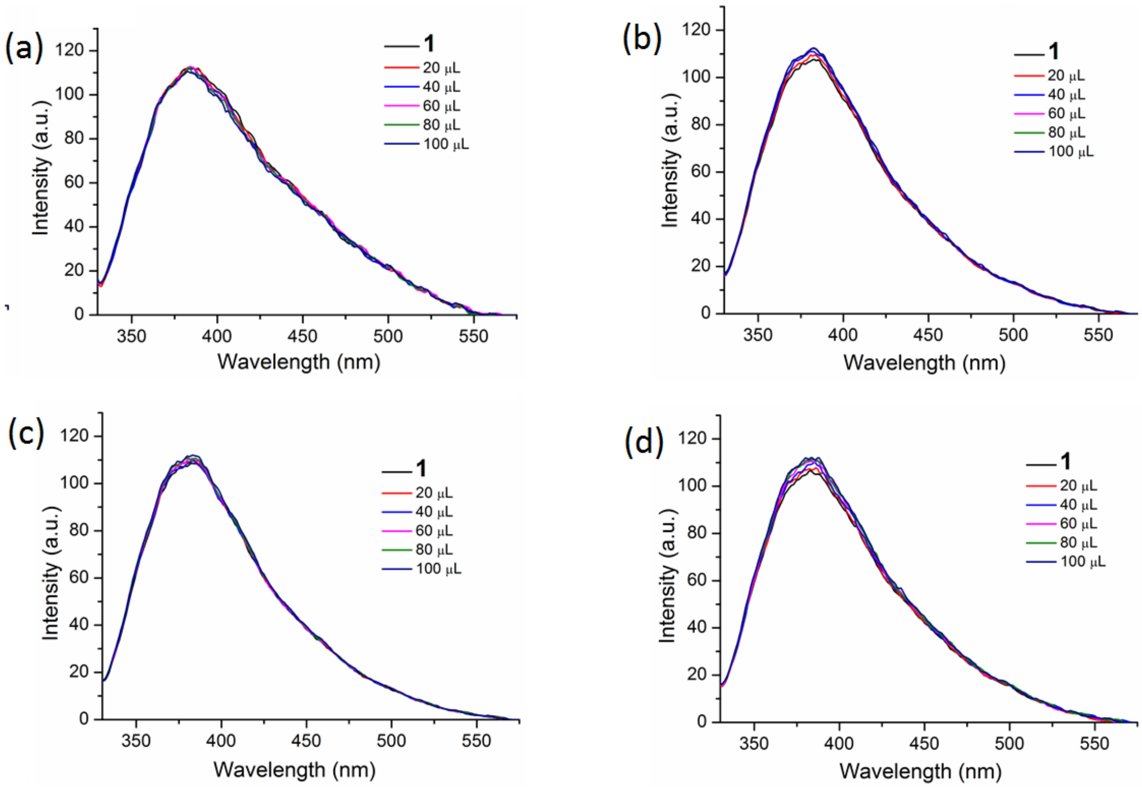

Fig. S17: The change in fluorescence intensity of **1** upon incremental addition of Catechol (**a**), 2,6 Bis(hydroxymethyl) p-cresol (**b**), di(trimethylolpropane) (**c**) and 1,1,1-Tris(hydroxymethyl)propane (**d**) (1mM) solution in Water.

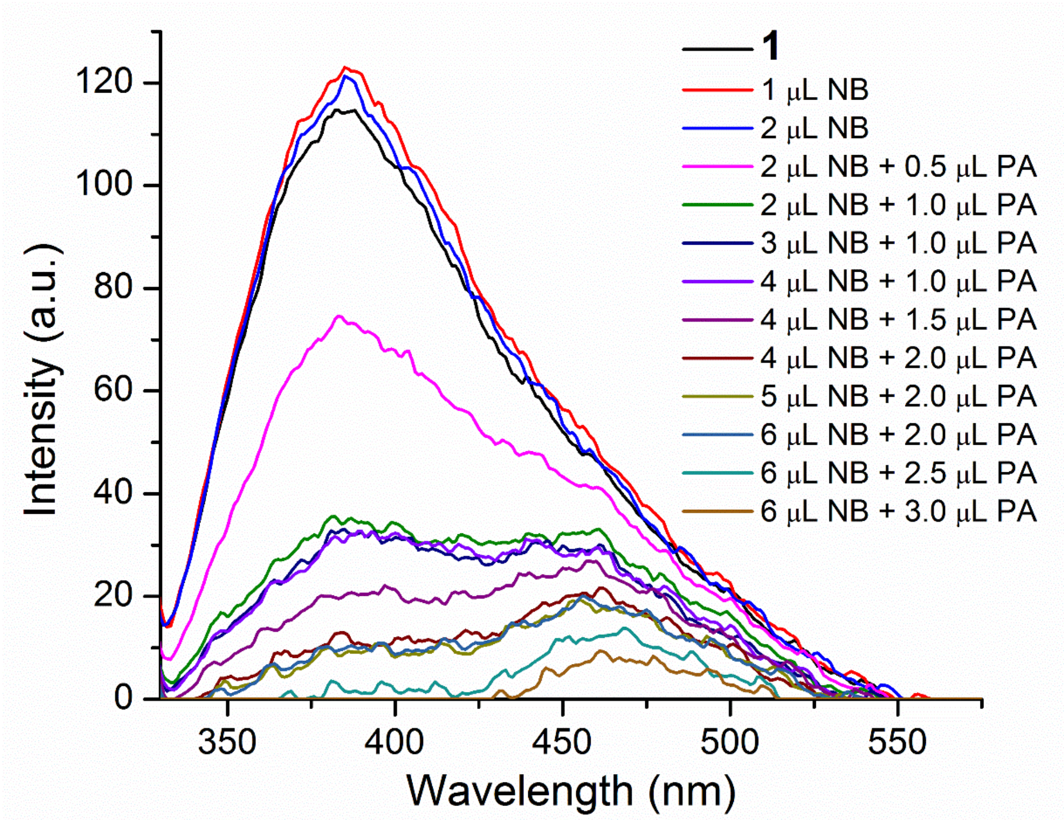

Fig. S18: The change in fluorescence intensity of **1** upon addition of NB followed by PA.

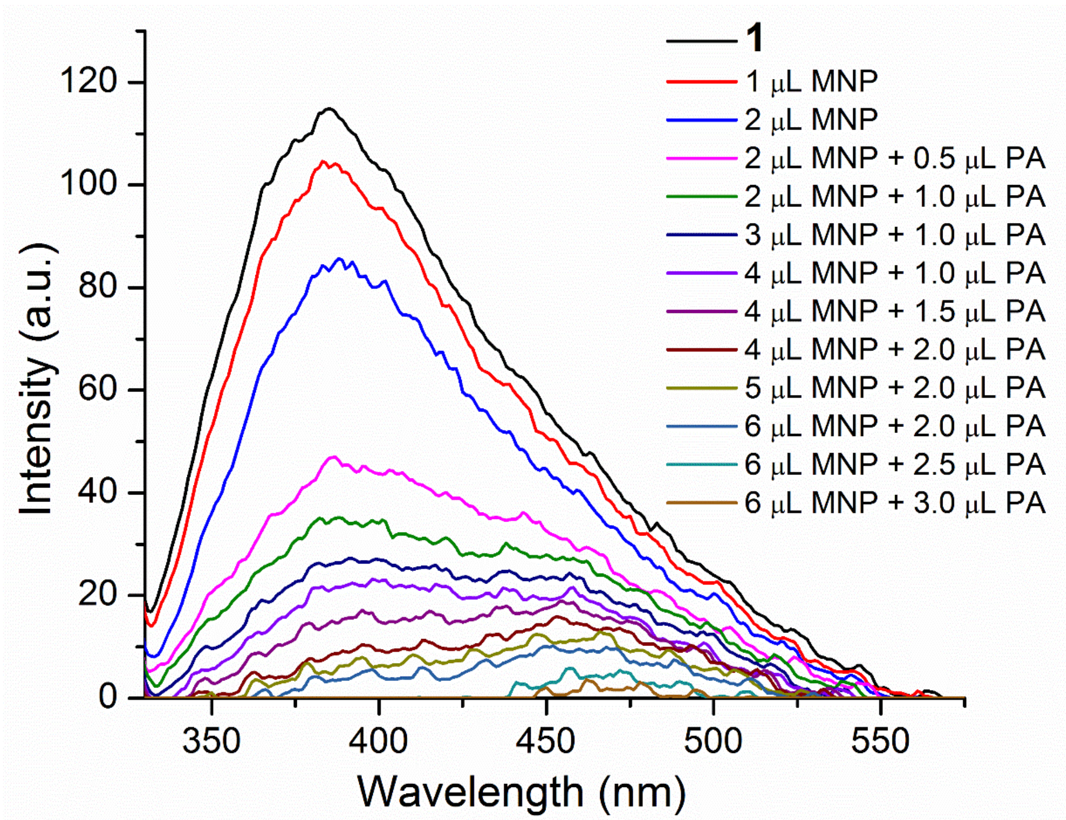

Fig. S19: The change in fluorescence intensity of **1** upon addition of MNP followed by PA.

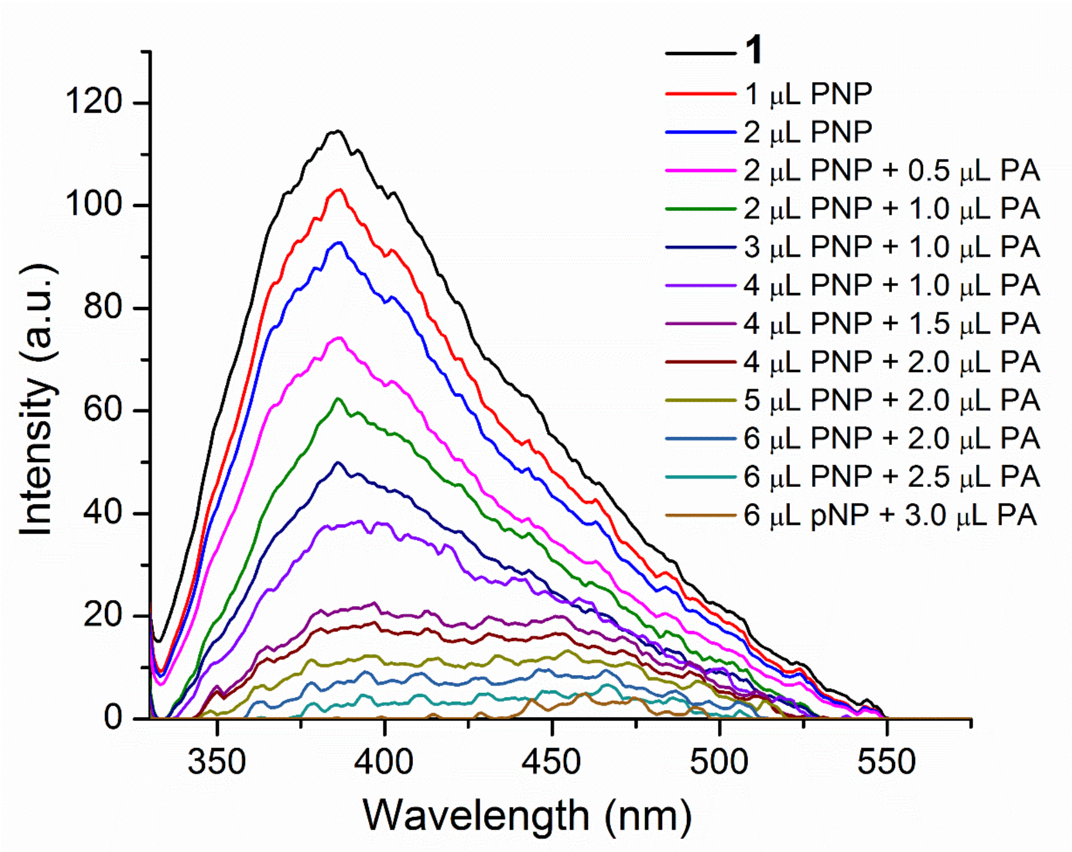

Fig. S20: The change in fluorescence intensity of **1** upon addition of PNP followed by PA.

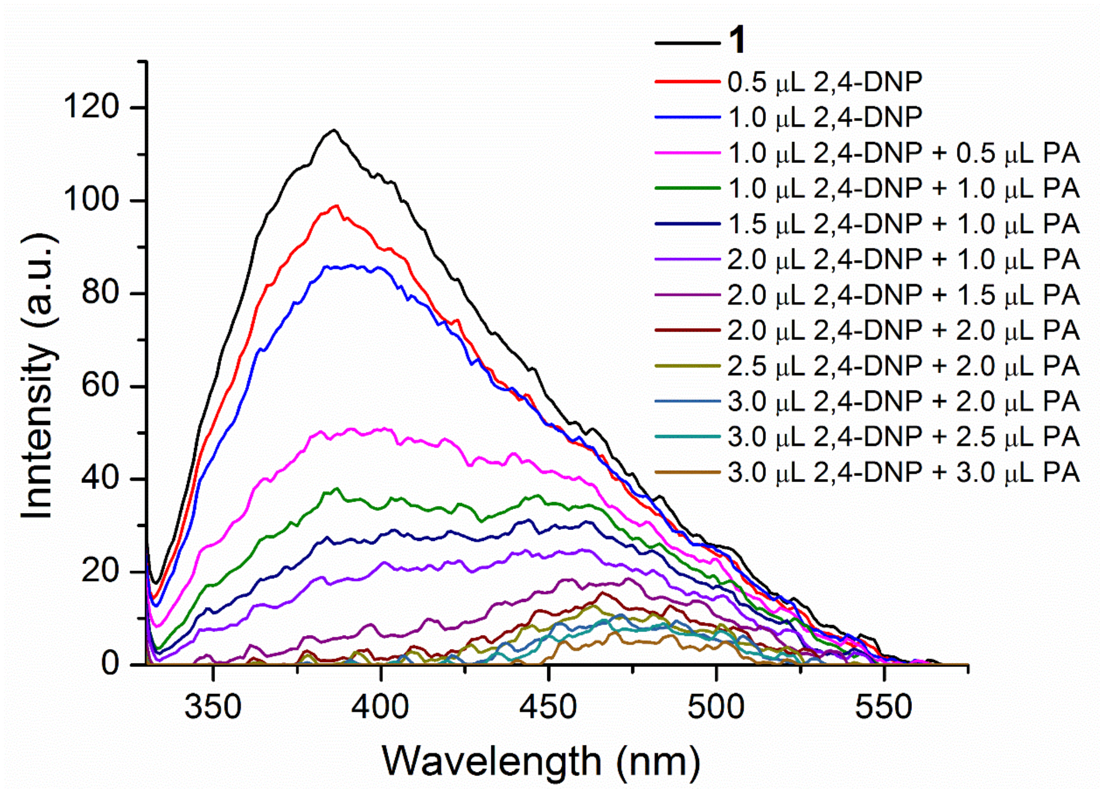

Fig. S21: The change in fluorescence intensity of **1** upon addition of 2,4-DNP followed by PA.

Table S3: - HOMO and LUMO energies calculated for nitroanalytes and ligand at B3LYP/6- 31G* level of theory.

Analytes	HOMO (ev)	LUMO (eV)	Band gap (eV)
NB	-7.752	-3.023	4.729
PNP	-7.236	-2.722	4.514
MNP	-7.029	-2.984	4.045
2,4-DNP	-6.408	-3.014	3.394
PA	-8.205	-4.384	3.821

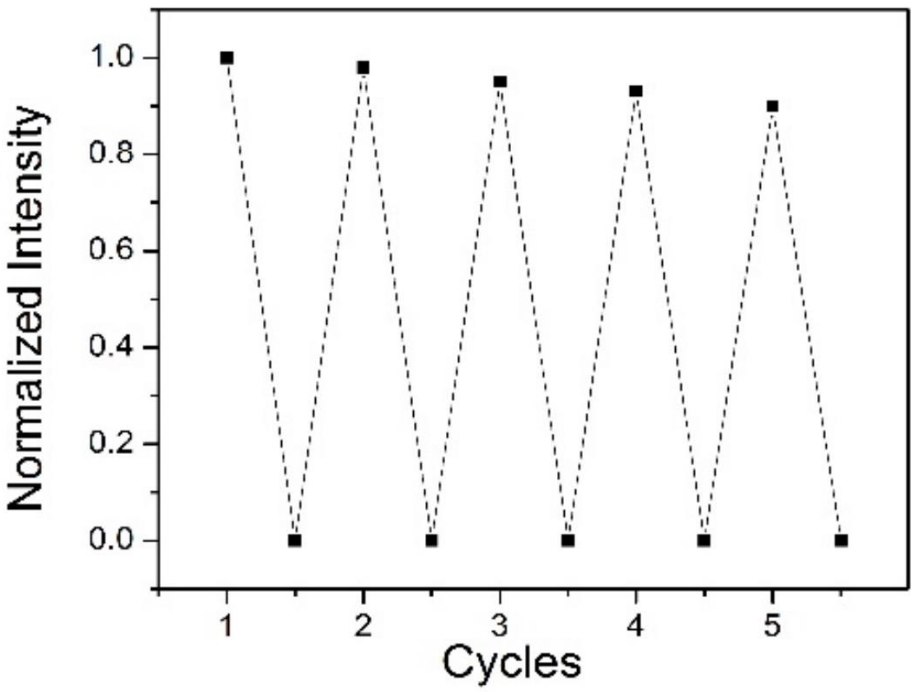

Fig. S22: The quenching and recyclability test of 1, the upper dots represent the initial luminescence intensity and the lower dots represent the intensity upon addition of 4.58ppb of PA solution.

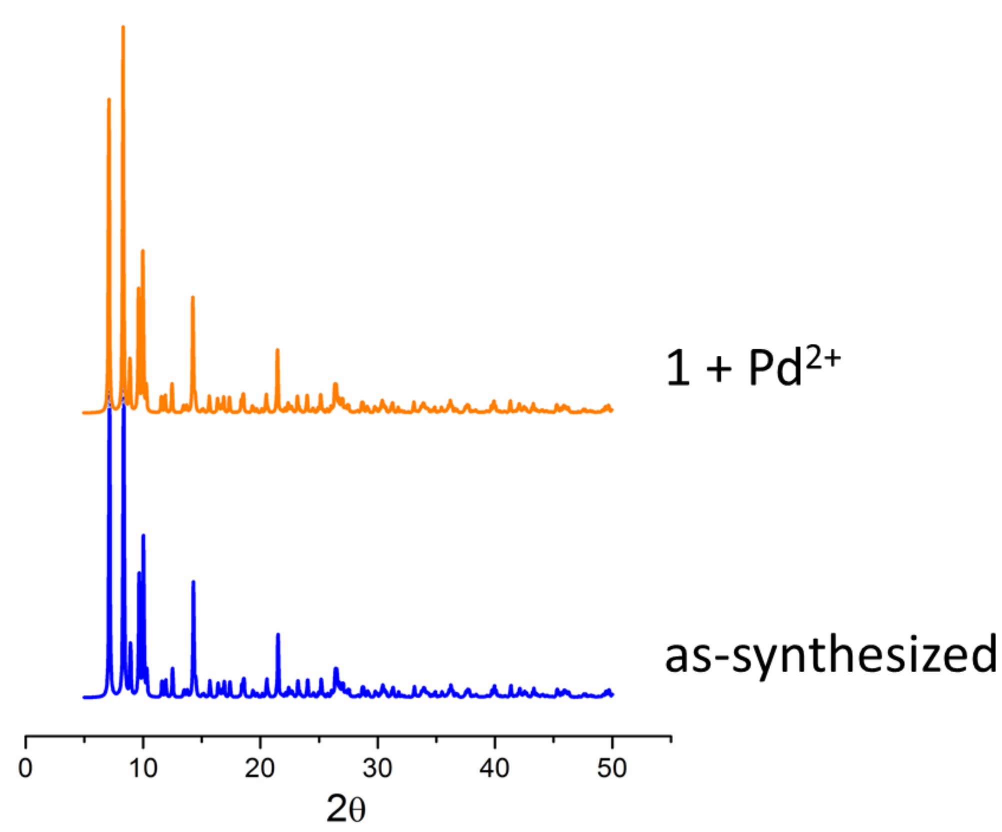

Fig. S23: PXRD patterns of **1**: as-synthesized (blue) and after immersion in Pd^{2+} solution for 12 hrs (orange).

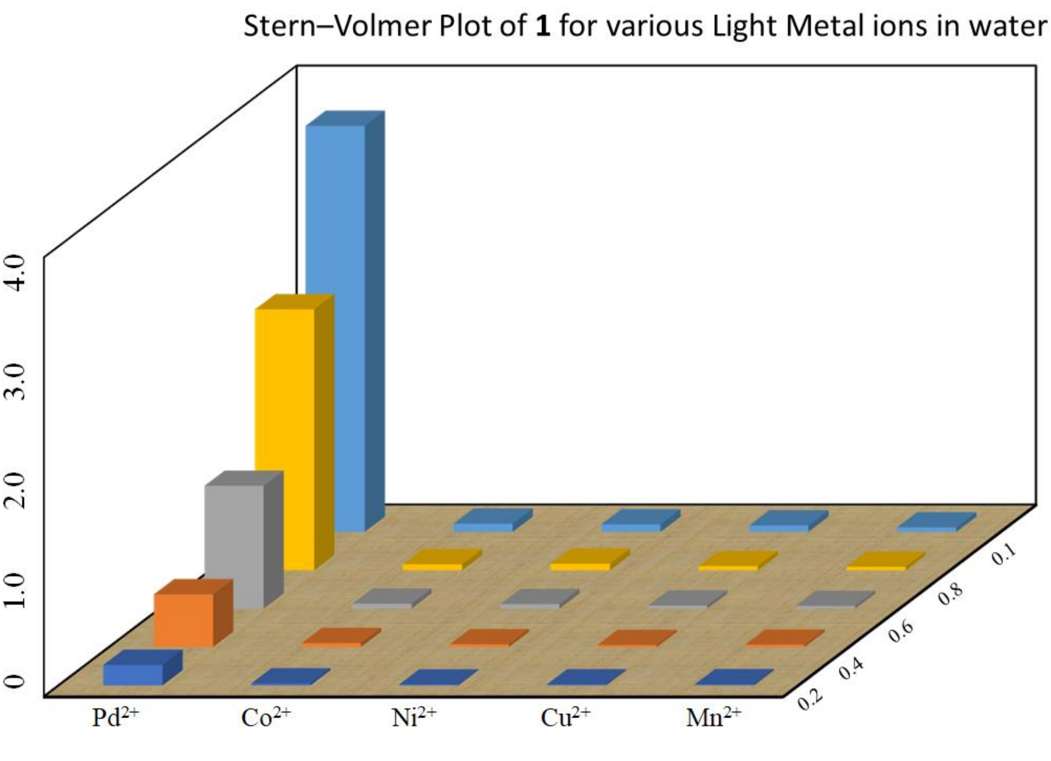

Fig. S24: 3D representation of Stern-Volmer (SV) plots of **1** for various light metal ions.

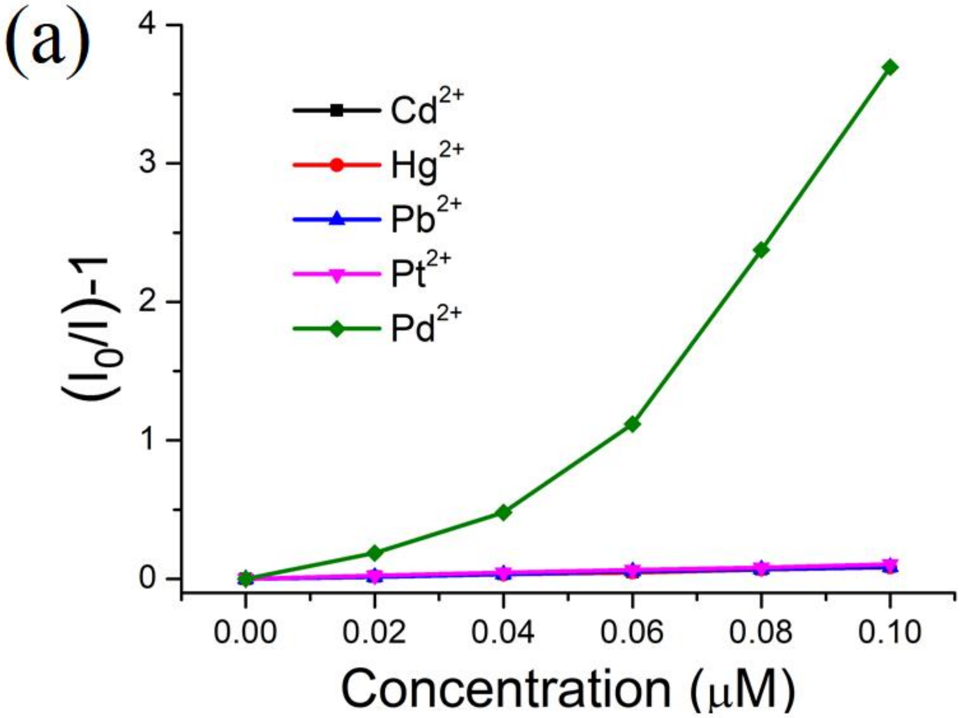

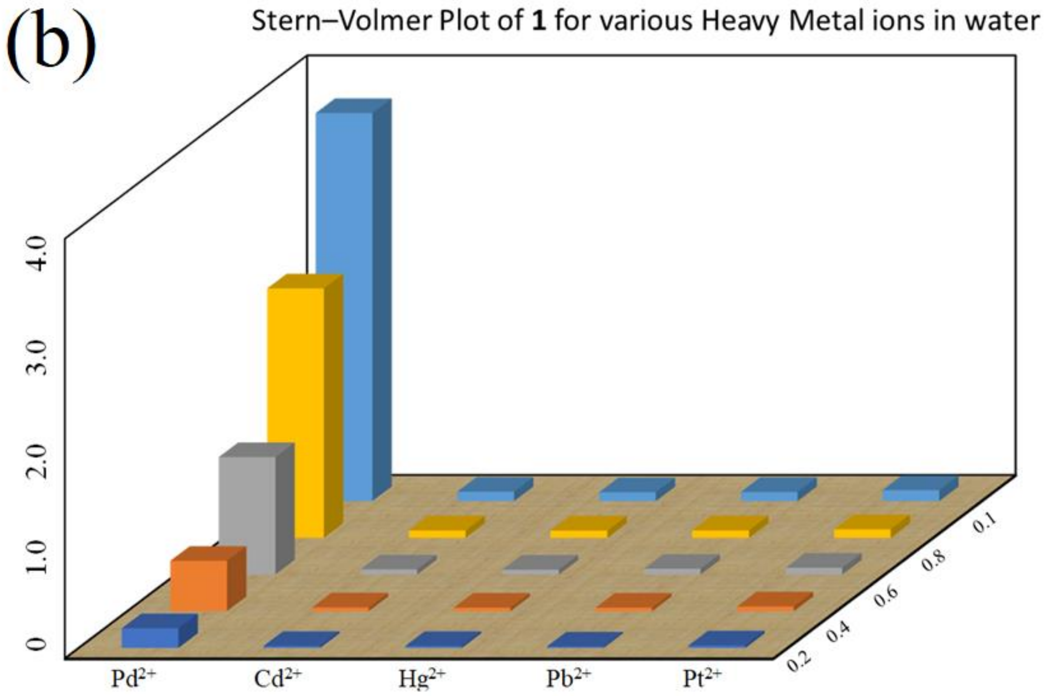

Fig. S25: (a) Stern–Volmer plot for various heavy analytes. (b) 3D representation of Stern-Volmer (SV) plots of **1** for various heavy metal ions.

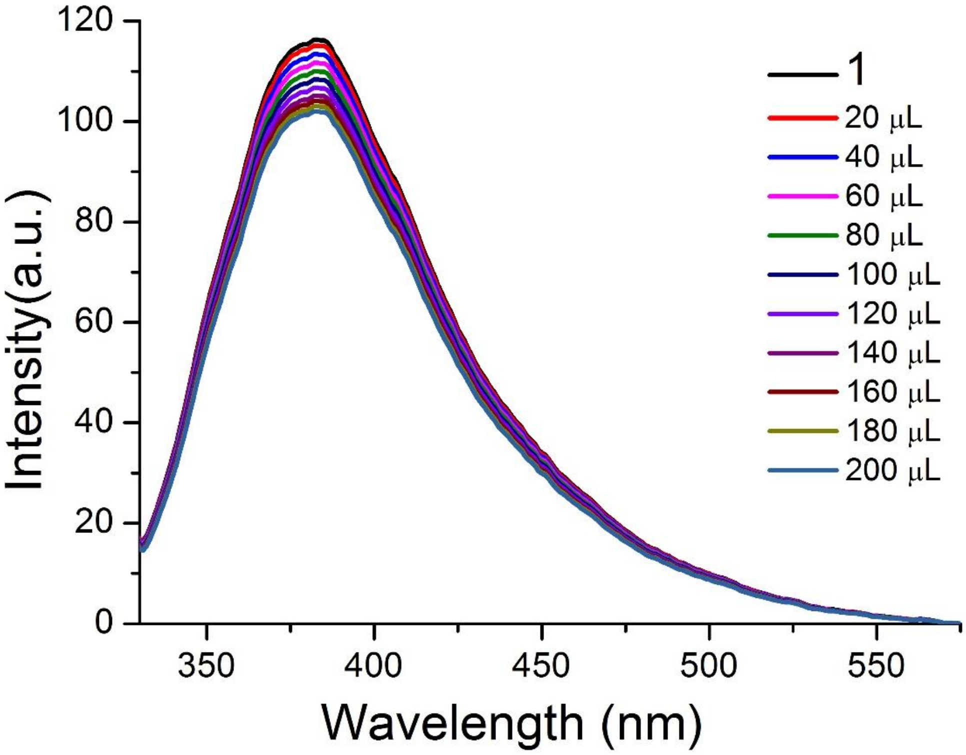

Fig. S26: Emission spectrum of **1** upon incremental addition of Co^{2+} (1mM) solution in Water.

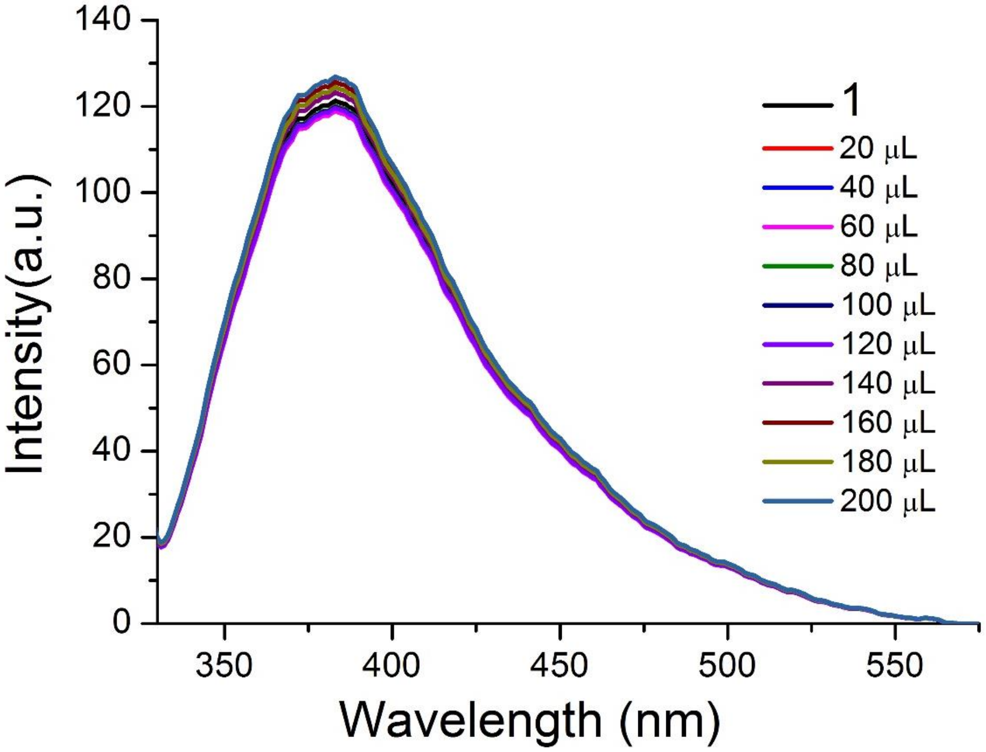

Fig. S27: Emission spectrum of **1** upon incremental addition of Ni^{2+} (1mM) solution in Water.

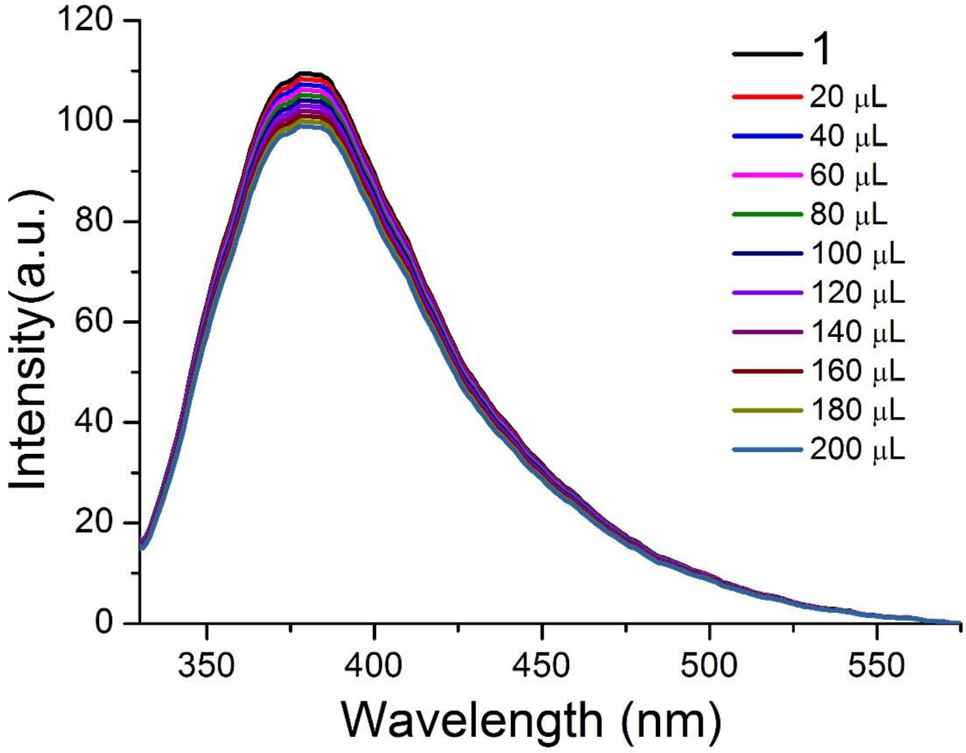

Fig. S28: Emission spectrum of **1** upon incremental addition of Cu^{2+} (1mM) solution in Water.

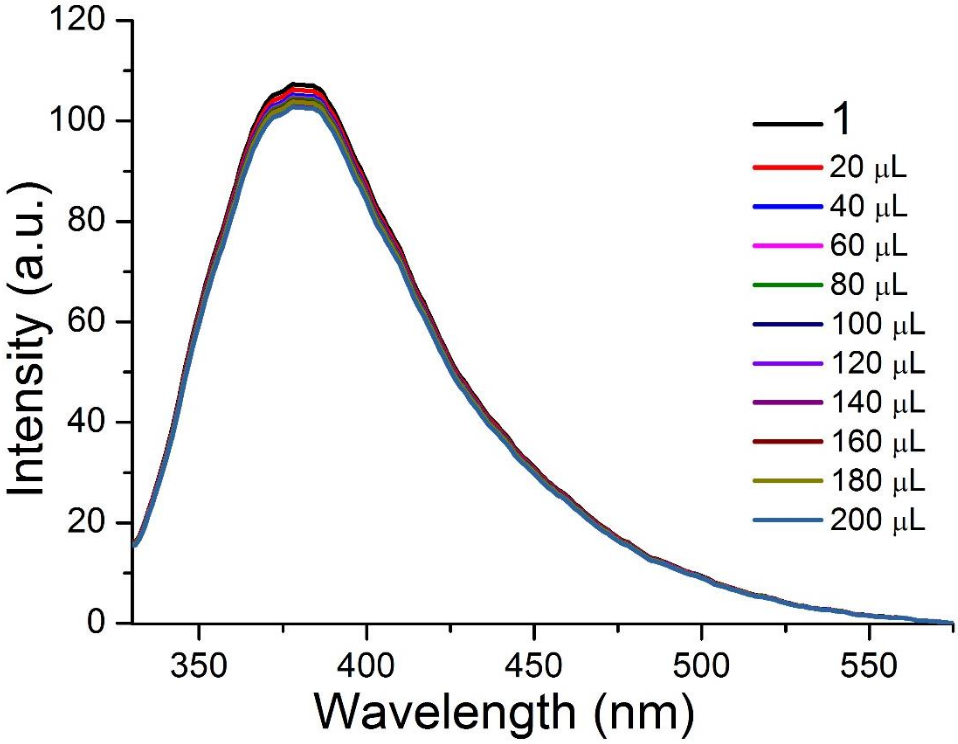

Fig. S29: Emission spectrum of **1** upon incremental addition of Mn^{2+} (1mM) solution in Water.

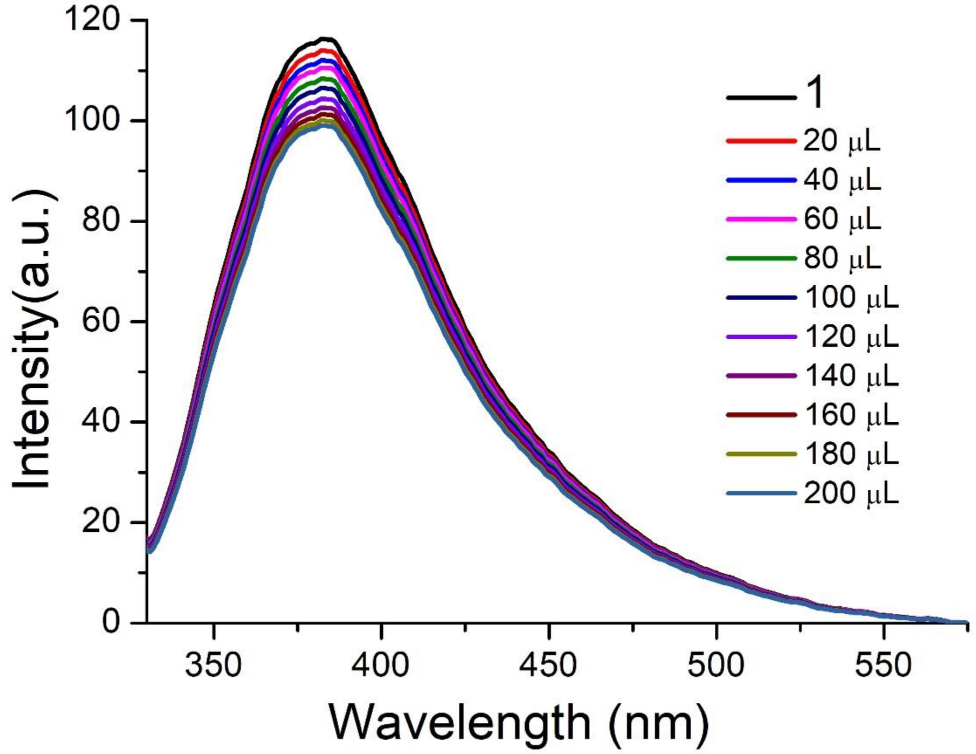

Fig. S30: Emission spectrum of **1** upon incremental addition of Cd^{2+} (1mM) solution in Water.

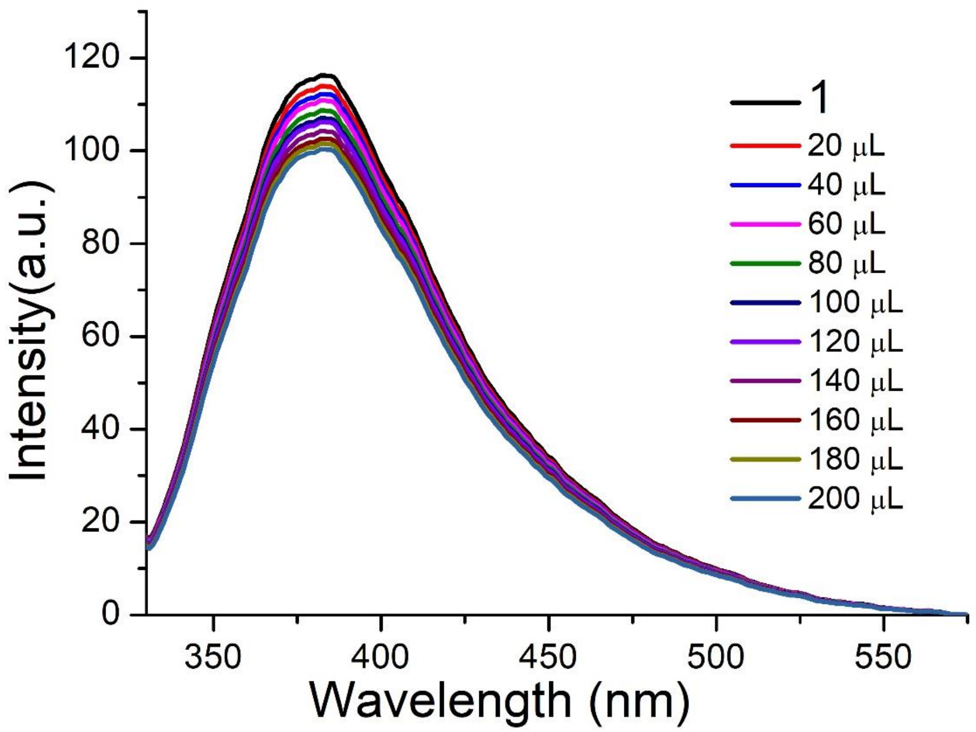

Fig. S31: Emission spectrum of **1** upon incremental addition of Hg^{2+} (1mM) solution in Water.

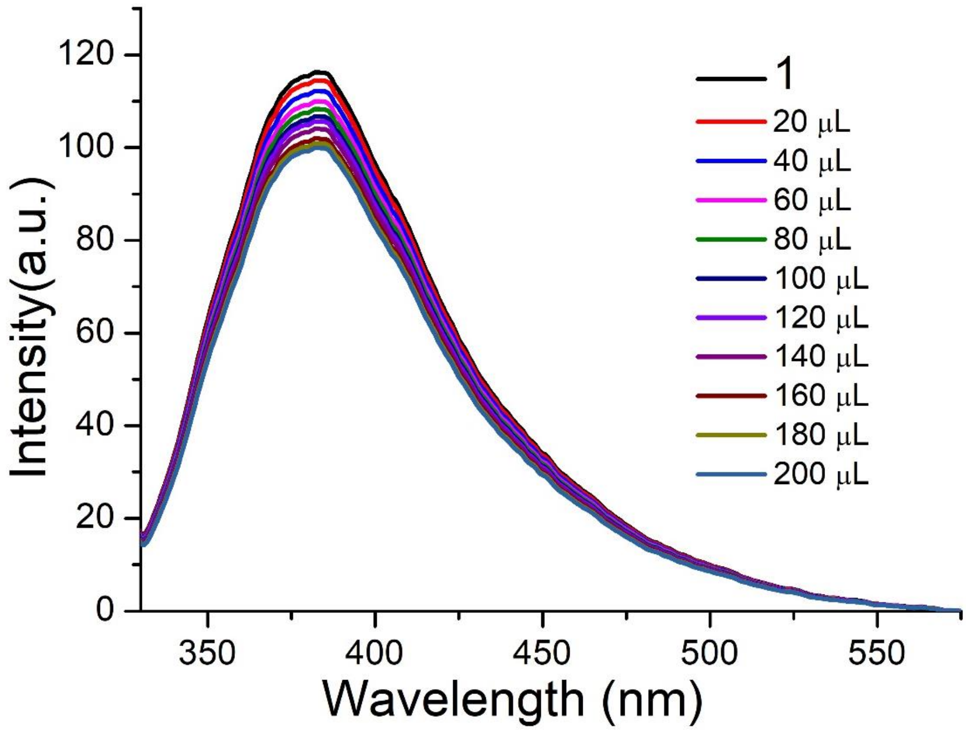

Fig. S32: Emission spectrum of **1** upon incremental addition of Pb^{2+} (1mM) solution in Water.

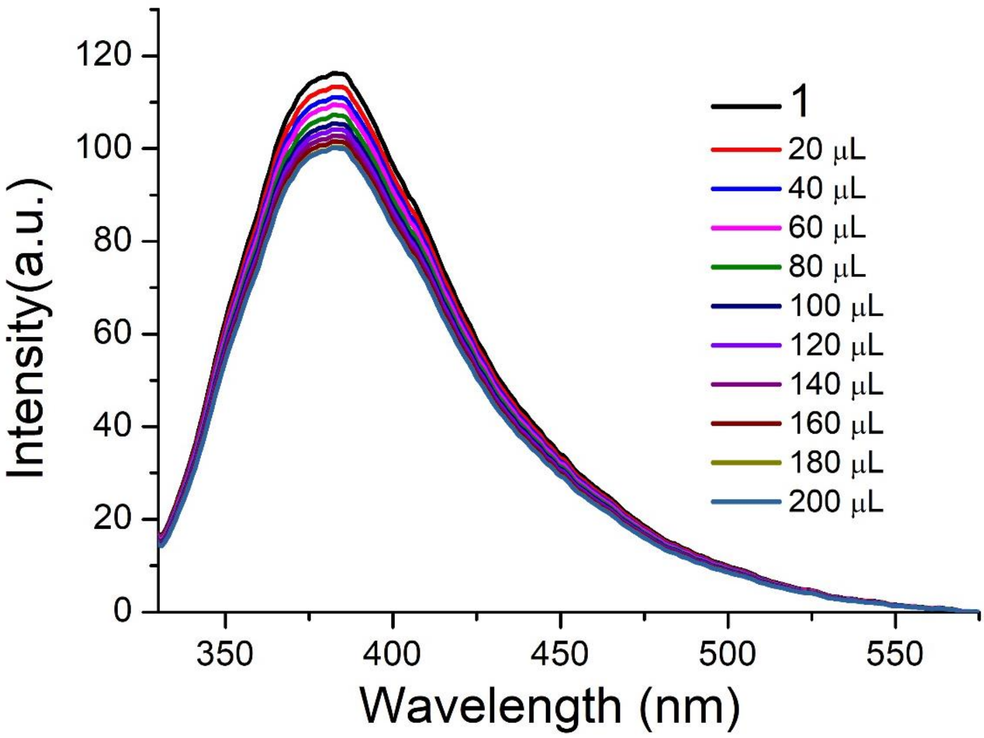

Fig. S33: Emission spectrum of **1** upon incremental addition of Pt^{2+} (1mM) solution in Water.

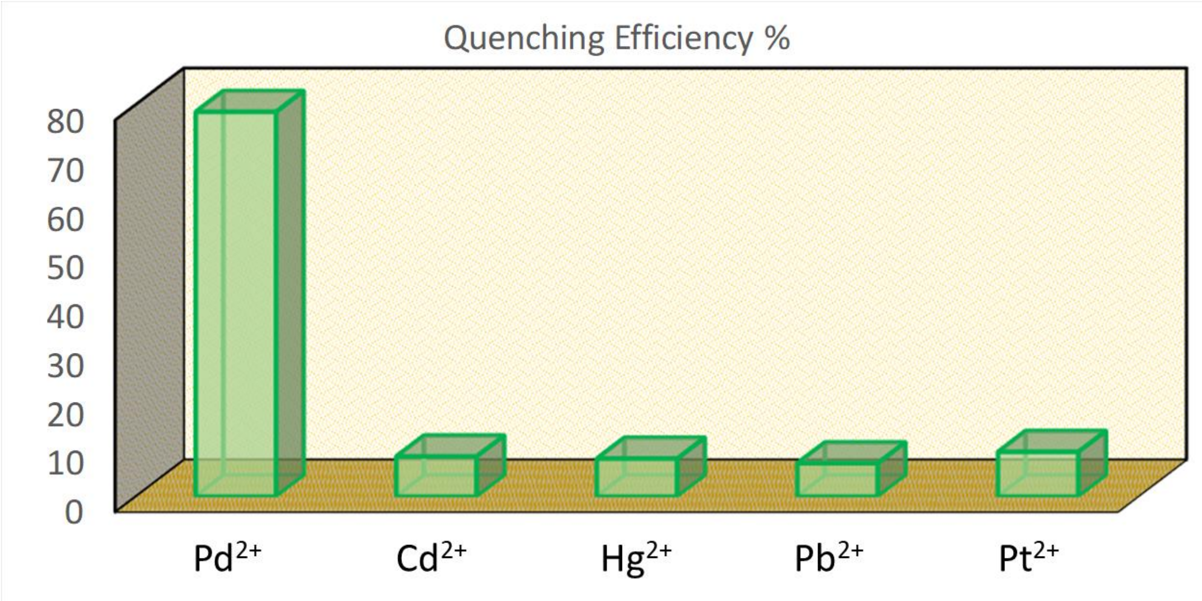

Fig. S34: The fluorescence quenching efficiencies of different analytes upon addition of 11 ppb.

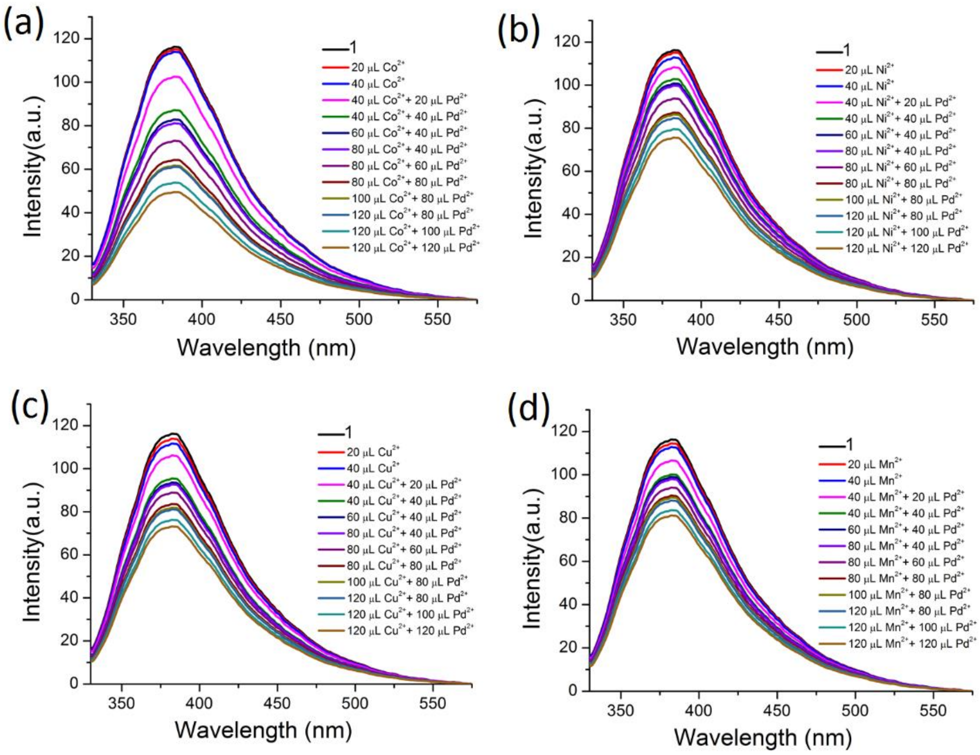

Fig. S35: The change in fluorescence intensity of **1** upon addition of Co^{2+}(a), Ni^{2+}(b), Cu^{2+}(c) and Mn^{2+}(d) solution followed by Pb^{2+} solution respectively.

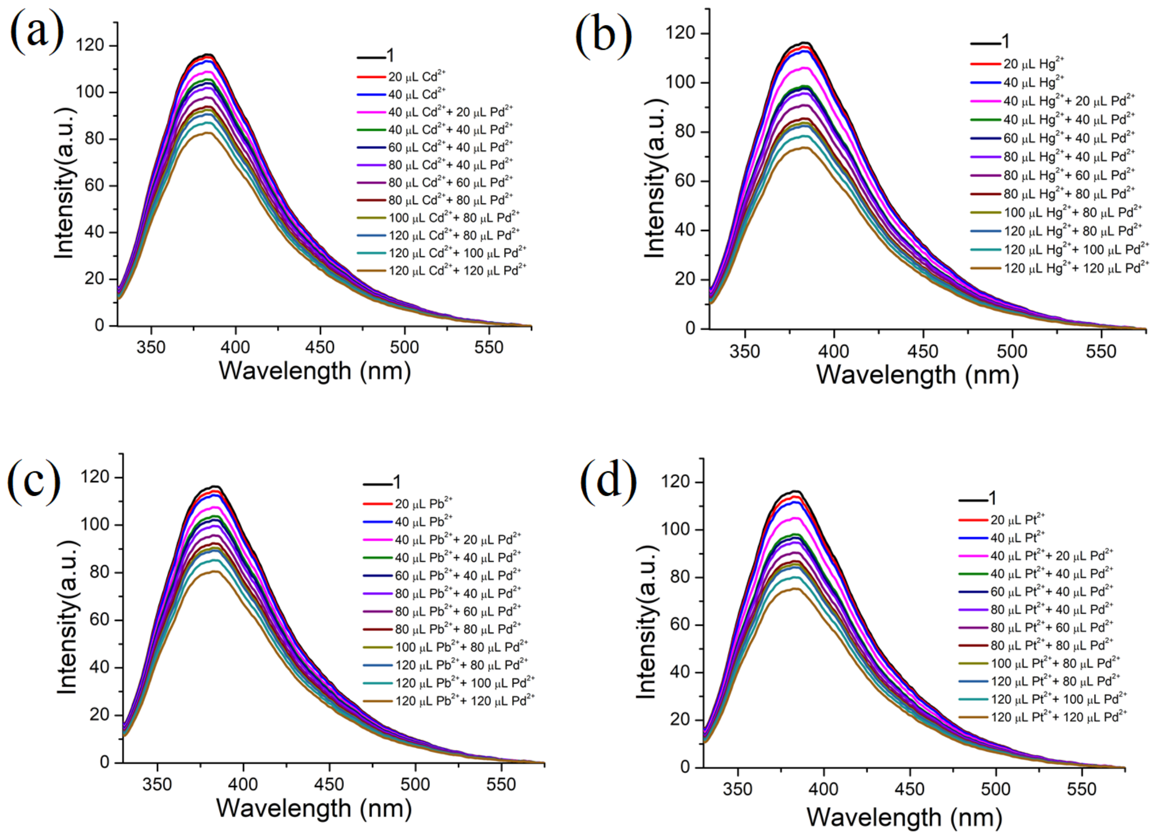

Fig. S36: The change in fluorescence intensity of **1** upon addition of Cd^{2+}(a), Hg^{2+}(b), Pb^{2+}(c) and Pt^{2+}(d) solution followed by Pb^{2+} solution respectively.

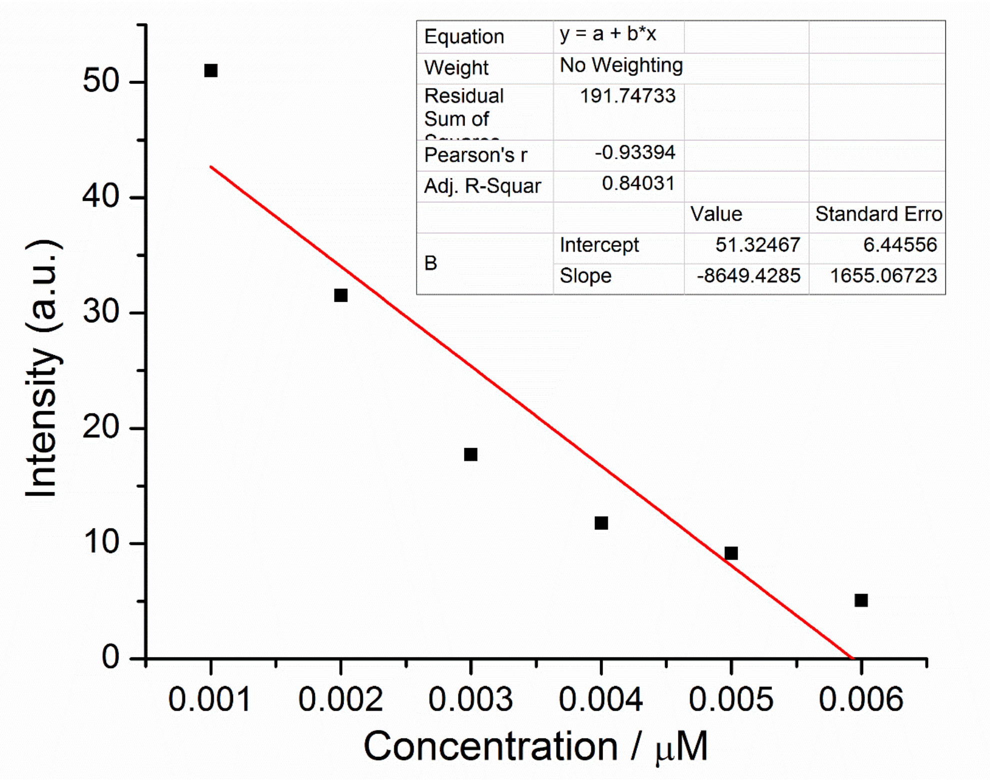

Fig. S37: Linear region of fluorescence intensity of **1** in water upon addition of PA (0.5 – 3 μL, 2 mM stock solution) in water.

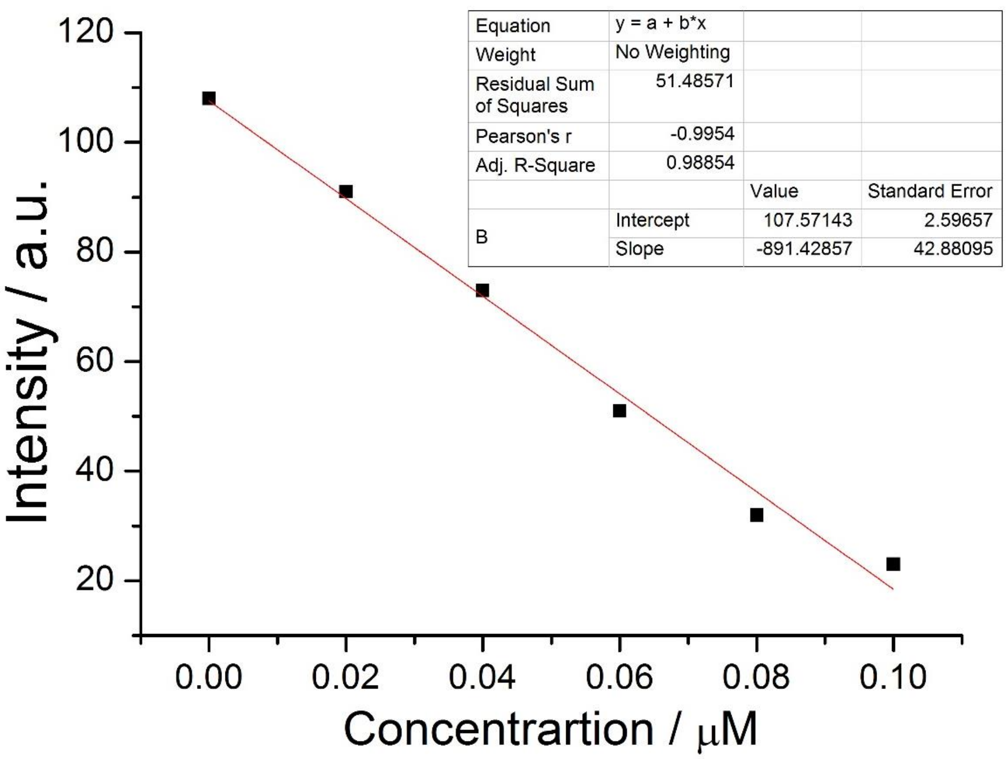

Fig. S38: Linear region of fluorescence intensity of **1** in water upon addition of Pd^{2+} (20 – 100 μL, 1 mM stock solution) in water.

Table S4. Selected bond lengths and angles for **1**.

Bond Length (**1**)			
O0AA–V6	1.766(6)	O15–V2	1.930(6)
O0AA–V10	1.923(6)	O15–V3	1.946(6)
O2–V6	1.949(6)	O15–V0AA	2.016(6)
O2–V8	2.026(6)	O16–V2	1.762(6)
O3 –V9	1.919(6)	O16 –V4	1.908(6)
O3 –V7	1.925(6)	O17 –V7	1.608(7)
O3–V6	2.072(6)	O18–V8	1.770(6)
O4–V9	2.112(6)	O18–V7	1.910(6)
O4–V6	2.268(6)	O19–V10	1.602(6)
O4–V7	2.283(6)	O20–V6	1.600(7)
O4 –V8	2.309(6)	O21 –V6	1.934(6)
O4 –V10	2.314(5)	O21 –V9	1.957(6)
O5–V9	1.681(6)	O21–V7	2.022(6)
O5–V10	2.074(6)	O22–V1	1.612(7)
O6–V9	1.702(6)	O23–V2	1.597(7)
O6–V8	2.022(6)	O24–V0AA	1.601(6)
O7 –V7	1.816(6)	O25 –V1	1.783(7)
O7 –V10	1.873(7)	O25 –V0AA	1.916(6)
O8–V10	1.795(6)	O26–V0AA	1.832(6)
O8–V8	1.853(6)	O26–V4	1.887(6)
O9–V3	1.706(6)	O27–V4	1.619(6)
O9–V1	2.018(6)	O28–V8	1.613(6)
O10 –V2	1.959(6)	O34 –Cu1	1.921(9)
O10 –V1	2.026(6)	O35 –Cu1	1.898(9)
O11–V0AA	1.931(6)	O37–Cu2	1.947(10)
O11–V3	1.933(6)	O38–Cu2	1.927(9)
O11–V2	2.058(6)	N1–O34	1.291(12)
O12–V3	2.117(6)	N2–O35	1.314(12)
O12 –V2	2.261(6)	N3 –O37	1.289(12)
O12 –V0AA	2.297(6)	C32 –N4	1.352(16)
O12–V1	2.301(6)	C27–N3	1.307(16)
O12–V4	2.315(5)	C28–N4	1.363(15)
O13–V3	1.680(6)	C24–N3	1.392(16)
O13–V4	2.075(6)	C1–N6	1.521(13)
O14 –V4	1.791(6)	C5 –N6	1.490(14)
O14 –V1	1.863(6)	C17 –N1	1.333(15)
Bond angles (1)			
V6 –O0AA –V10	114.8(3)	V3 –O11 –V2	108.9(3)
V6 –O2 –V8	112.2(3)	V3 –O12 –V3	100.9(2)
V9 –O3 –V7	108.3(3)	V2 –O12 –V0AA	170.6(3)
V9 –O3 –V6	108.2(3)	V3 –O12 –V1	170.7(3)
V7 –O3 –V6	98.0(3)	V2 –O12 –V1	92.8(2)
V9 –O4 –V6	91.0(2)	V3 –O12 –V4	170.5(3)
V9 –O4 –V7	90.3(2)	V2 –O12 –V4	85.42(19)
V6 –O4 –V7	170.5(3)	V3 –O13 –V4	110.6(3)
V9 –O4 –V8	170.9(3)	V3 –O14 –V1	114.1(3)
V6 –O4 –V8	92.3(2)	V2 –O15 –V3	107.1(3)
V7 –O4 –V8	85.17(19)	V2 –O16 –V4	115.5(3)
V9 –O4 –V8	88.6(2)	N1 –O34 –Cu1	121.2(7)
V9 –O5 –V10	110.6(3)	N4 –O38 –Cu2	121.4(8)
V9 –O6 –V8	110.0(3)	O35 –Cu1 –O34	90.1(4)
V7 –O7 –V10	115.0(3)	O38 –Cu2 –O37	90.3(4)
V10 –O8 –V8	114.5(3)	N3 –O37 –Cu2	119.8(7)
V3 –O9 –V1	110.1(3)	N4 –O38 –Cu2	121.4(8)
V2 –O10 –V1	112.0(3)	O34 –Cu1 –O34	180.000(2)
V0AA –O11 –V3	108.0(3)	O38 –Cu2 –O38	180.0(7)

Calculation of standard deviation:

Table S5: Standard deviation for **1**.

Blank Readings (only probe)	FL Intensity of **1**
Reading 1	111.03
Reading 2	110.26
Reading 3	109.04
Reading 4	107.50
Reading 5	114.49
Standard Deviation (σ)	**2.34**

Calculation of Detection Limit:

Table S6: Detection limit calculation of **1** for PA

Complex	Slope from Graph (m)	Detection limit (3σ/*m*)	
		μM	ppb
1	8649.43	8.12E-04	~0.18

Table S7: Detection limit calculation of **1** for Pd^{2+}

Complex	Slope from Graph (m)	Detection limit (3σ/*m*)	
		μM	ppb
1	891.42	7.88E-03	~0. 80